IL NUOVO CIMENTO **40 C** (2017) 83
DOI 10.1393/ncc/i2017-17083-8

COMMUNICATIONS: SIF Congress 2016

D-meson reconstruction in pp collisions at $\sqrt{s} = 8\,\text{TeV}$ with the ALICE experiment at LHC

S. COSTANZA(1)(2) on behalf of the ALICE COLLABORATION

(1) *Dipartimento di Fisica, University of Pavia - Pavia, Italy*
(2) *INFN, Sezione di Pavia - Pavia, Italy*

received 28 February 2017

Summary. — The study of the production of hadrons containing heavy quarks (charm and beauty) in proton-proton (pp) collisions at LHC energies is a very important test of perturbative Quantum Chromodynamics (pQCD). In this paper, we report about the production cross section of prompt charmed D^{*+} and D^{+} mesons, measured at mid-rapidity in proton-proton collisions at a centre-of-mass energy $\sqrt{s} = 8\,\text{TeV}$ with the ALICE detector at the Large Hadron Collider (LHC). The D mesons are reconstructed in their hadronic decay channels $\mathrm{D}^{*+} \to \mathrm{D}^0\pi^+$, $\mathrm{D}^0 \to \mathrm{K}^-\pi^+$ and $\mathrm{D}^+ \to \mathrm{K}^-\pi^+\pi^+$, and their charge conjugates. The reconstruction procedure, the raw yield extraction and the corrections applied to obtain the production cross section are presented. The measured p_T differential cross sections are then compared to QCD predictions.

1. – Introduction

The production of heavy quarks in high-energy hadronic collisions, such as proton-proton collisions at LHC energies, can be described in the framework of Quantum Chromodynamics: cross sections can be factorised as a convolution of the parton distribution functions (PDFs) of the incoming hadron, the partonic hard-scattering cross sections and the fragmentation functions of the heavy quarks hadronising to a particular species of heavy-flavour hadron.

The production cross sections of D and B mesons in proton-proton (and proton-antiproton) collisions at the centre-of-mass energies from 0.2 to 13 TeV, in a wide p_T range at both central and forward rapidity are reproduced by state-of-the-art calculations, such as FONLL [1, 2] and GM-VFNS [3-5], within uncertainties. Furthermore, the measurements of charm production in the low p_T region is particularly sensitive to the gluon PDFs at small values of proton fractional momentum x and squared momentum transfer Q^2, where they are not well constrained by data. This strongly motivates the measurement of D-meson production in pp collisions at LHC energies.

Moreover, within the LHC heavy-ion programme, the D-meson production cross section in pp collisions is used as an essential reference for the study of effects induced by strongly-interacting matter in the case of nucleus-nucleus collisions.

In this article, we report about the measurement of the production cross section of the prompt charmed D^+ and D^{*+} mesons (as average of particles and antiparticles), in pp collisions at the centre-of-mass energy $\sqrt{s} = 8\,\mathrm{TeV}$, using data collected with the ALICE detector at LHC in 2012. The measurements cover mid-rapidity ($|y| < 0.5$) and a p_T range from 1 to $24\,\mathrm{GeV}/c$.

The detector layout and the data sample used in the analysis are described in sect. **2**, the D-meson reconstruction and selection strategy are reported in sect. **3**, and the correction factors to the cross sections and the systematic uncertainties are detailed in sect. **4**. Finally, the cross section results are presented and compared to theoretical calculations in sect. **5**.

2. – Apparatus and data sample

The ALICE apparatus [6,7] consists of a central barrel with a set of detectors devoted to tracking and particle identification, covering the pseudorapidity region $|\eta| < 0.9$, located within a large solenoidal magnet that provides a magnetic field $B = 0.5\,\mathrm{T}$ parallel to the beam direction (z-axis of the ALICE reference frame). The central barrel is complemented by a muon spectrometer in the forward direction for muon identification and reconstruction, and by additional series of detectors in the forward and backward regions for trigger and event characterisation.

D mesons were reconstructed at mid-rapidity from their decay products, with the tracking and particle identification detectors of the ALICE central barrel.

In this section, the detectors used for the D-meson analysis are briefly described: the Inner Tracking System (ITS), the Time Projection Chamber (TPC), the Time Of Flight detector (TOF), which are dedicated to the charged particle reconstruction and identification in the pseudorapidity region $|\eta| < 0.9$, and the V0 detector, consisting of two scintillator arrays ($-3.7 < \eta < -1.7$ and $2.8 < \eta < 5.1$) and used for online triggering and multiplicity determination [8].

The innermost detector of the ALICE apparatus is the ITS: it consists of six cylindrical layers of silicon detectors, located at radii between 3.9 cm ($\sim 1\,\mathrm{cm}$ from the beam vacuum tube) and 43.0 cm. It is equipped with Silicon Pixel Detectors (SPD, two innermost layers), Silicon Drift Detectors (SDD, two intermediate layers) and Silicon Strip Detectors (SDD, two outermost layers). Thanks to the low material budget, the high spatial resolution and the proximity of the detector to the interaction point, the ITS is able to provide a resolution on the charged-track impact parameter d_0 in the transverse plane (distance of closest approach between the track and the primary vertex along $r\phi$) better than $75\,\mu\mathrm{m}$ for transverse momenta $p_\mathrm{T} > 1\,\mathrm{GeV}/c$ [9].

The ITS is surrounded by a large cylindrical TPC [10], with a radial distance to the beamline from 85 cm to 247 cm and an active length of 500 cm along the beam axis. It provides track reconstruction with up to 159 three-dimensional space-points per track, as well as particle identification by measuring the specific energy loss $\mathrm{d}E/\mathrm{d}x$.

The charged particle identification capabilities of the TPC are extended by the TOF detector, which is equipped with Multi-gap Resistive Plate Chambers (MRPCs) placed at radii between 377 cm and 399 cm. It measures the flight time of the particles from the interaction point to the detector with a resolution of about 85 ps. The start time of an event can be determined by using the arrival time of the particles at the TOF detector,

for events with a sufficiently large multiplicity, or it can be measured by the T0 detector, consisting of two arrays of Cherenkov counters located at +350 cm and −70 cm along the beam line [11].

The data sample used for the analyses presented in this paper was recorded during the 2012 LHC run with pp collisions at $\sqrt{s} = 8$ TeV. A minimum-bias (MB) trigger was used to collect the data, by requiring at least one hit in both of the V0 counters. The number of events passing the selection criteria was about 100 millions, corresponding to an integrated luminosity of $L_{\rm int} = (1.9 \pm 0.1)\,{\rm nb}^{-1}$ (sect. **4**˙1).

3. – Analysis procedure

3˙1. *Reconstruction of D-meson decays.* – $\rm D^+$ and $\rm D^{*+}$ mesons, as well as their antiparticles, were reconstructed in the central rapidity region via their hadronic decay channels $\rm D^+ \to K^-\pi^+\pi^+$, with branching ratio BR = $(9.13 \pm 0.19)\%$, and $\rm D^{*+} \to D^0\pi^+$, strong decay with BR = $(67.7 \pm 0.5)\%$, with $\rm D^0 \to K^-\pi^+$, with BR = $(3.93 \pm 0.04)\%$.

D-meson candidates were reconstructed from triplets of tracks with the proper charge-sign combination; in addition, they were required to have $\eta < |0.8|$, $p_{\rm T} > 0.3\,{\rm GeV}/c$, at least 70 (out of a maximum of 159) associated TPC space-points and a $\chi^2/{\rm ndf} < 2$ in the TPC (ndf is the number of degrees of freedom involved in the tracking procedure). Furthermore, at least one associated hit in either one of the two pixel layers was required, except for the soft pion produced in $\rm D^{*+}$ decay.

Additional $p_{\rm T}$-dependent kinematic and topological selections were applied on the final decay products to reduce combinatorial background and were optimized in order to ensure a large statistical significance.

Since the $\rm D^{*+}$-mesons decay strongly and their decay length at the primary vertex is too short, the geometrical cuts were applied on the $\rm D^0$ meson produced in the $\rm D^{*+}$-meson decay. The geometrical selections were based on the displacement of the reconstructed tracks from the interaction vertex (distance of closest approach, dca), the cosine of the pointing angle ($\cos\theta_{\rm pointing}$) between the reconstructed $\rm D^0$ momentum and the $\rm D^0$ flight line, and the product of impact parameters from the kaon and the pion ($d_0^K d_0^\pi$).

An additional selection criteria was used for the $\rm D^+$-meson case: a cut on the normalised difference between the measured and expected impact parameters of each of the decay particles $(d^{\rm reco}_{0,\,tr} - d^{\rm exp}_{0,\,tr})/\sigma_\Delta$ was applied. The measured track impact parameter is $d^{\rm reco}_{0,\,tr}$, $d^{\rm exp}_{0,\,tr}$ is defined as $L^{r\phi}\sin(\theta^{r\phi}_{\rm tr,\,D})$, where L is the decay length and $\theta^{r\phi}_{\rm tr,\,D}$ is the measured angle between the momenta of the D meson and of the considered track, and σ_Δ is the square root of the quadratic sum of the errors on $d^{\rm reco}_{0,\,tr}$ and $d^{\rm exp}_{0,\,tr}$. By applying this cut, it was possible to significantly reject background candidates and feed-down D mesons originating from decays of B mesons.

3˙2. *Signal extraction.* – The D-meson raw signal yields, including both particles and antiparticles, were extracted from fits to the $\rm D^+$-meson candidate invariant mass distributions and to the mass difference $\Delta M = M({\rm K}\pi\pi) - M({\rm K}\pi)$ distributions for the $\rm D^{*+}$-meson candidates. The distributions are shown in fig. 1 for $\rm D^+$ (top) and $\rm D^{*+}$ mesons (bottom) for three $p_{\rm T}$ intervals.

The invariant mass distributions were fitted with a Gaussian function for modeling the signal and an additional term to model the background: in case of $\rm D^+$-candidates, the background was described by an exponential function, while in case of $\rm D^{*+}$-candidates the function $a\sqrt{\Delta M - m_\pi}\exp(b(\Delta M - m_\pi))$ was used.

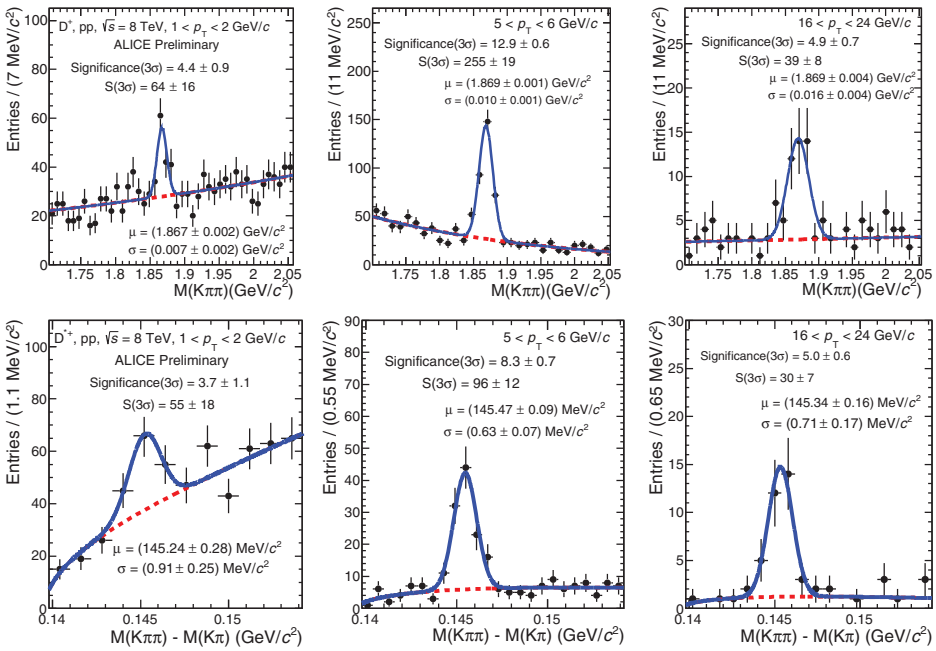

Fig. 1. – Invariant mass distributions for D^+-meson candidates (top) and mass-difference distributions for D^{*+}-meson candidates (bottom), for three p_T intervals in pp collisions at $\sqrt{s} = 8$ TeV. The curves show the fit functions as described in the text (sect. **3**˙2). The value of the mean (μ) of the signal peak and the signal counts (S) are reported in the mass interval $(\mu - 3\sigma, \mu + 3\sigma)$, where σ is the peak width.

The mean and width of the Gaussian fits from the data were compared in all p_T intervals with the results obtained from the Monte Carlo simulations: the mean values obtained from the analysis were found to be consistent with the world rest mass for D^+ mesons and with the mass difference D^{*+}-D^0 for D^{*+} mesons [12]. The widths of the fits for data and MC were compatible within statistical fluctuations.

4. – Correction factors and systematic uncertainties

4˙1. *Correction factors.* – The p_T differential production cross section for prompt charmed mesons, as average of particles and antiparticles, was obtained by using:

$$\left.\frac{\mathrm{d}\sigma^D}{\mathrm{d}p_T}\right|_{|y|<0.5} = \frac{1}{\Delta y \Delta p_T}\frac{1}{\mathrm{BR}}\frac{\frac{1}{2} f_{\mathrm{prompt}}(p_T)\cdot N^{\mathrm{D,raw}}(p_T)|_{|y|<y_{\mathrm{fid}}}}{(\mathrm{Acc}\times\epsilon)_{\mathrm{prompt}}(p_T)}\frac{1}{L_{\mathrm{int}}}, \quad (1)$$

where $N^{\mathrm{D,raw}}(p_T)$ is the measured inclusive raw yield extracted in each p_T bin (with width Δp_T) from the invariant mass plots, which contains both particles and antiparticles; this is taken into account by the factor 1/2, since the cross section is given only for particles.

In eq. 1, the factor f_{prompt} is the prompt fraction of the raw yield, used for correcting for the contribution from feed-down D mesons; $(\mathrm{Acc}\times\epsilon)_{\mathrm{prompt}}$ is the acceptance-times-efficiency for prompt D mesons, BR is the branching ratio of the decay channel, Δy $(= 2y_{\mathrm{fid}})$ is the width of the fiducial rapidity coverage, and L_{int} is the integrated luminosity.

The raw yield values were corrected for the B-meson decay feed-down contribution, *i.e.* multiplied by $f_{\rm prompt}$. This factor was estimated by using the beauty production cross section from the FONLL calculations [1, 2], the kinematics of the reaction B $\rightarrow$ D + X from the EvtGen package [13] and the Monte Carlo efficiencies for feed-down D mesons:

$$f_{\rm prompt} = 1 - \frac{N_{\rm raw}^{\rm D\ feed\text{-}down}}{N_{\rm raw}^{\rm D}} = 1 - \left(\frac{{\rm d}^2\sigma}{{\rm d}y{\rm d}p_{\rm T}}\right)^{\rm FONLL}_{\rm feed\text{-}down} \cdot \frac{({\rm Acc}\times\epsilon)_{\rm feed\text{-}down}\cdot\Delta y\Delta p_{\rm T}\cdot BR\cdot L_{\rm int}}{N^{\rm D\ raw}/2}. \tag{2}$$

In the equation, the $p_{\rm T}$-dependence of $f_{\rm prompt}$, $N^{\rm D,raw}$ and $({\rm Acc}\times\epsilon)_{\rm feed\text{-}down}$ has been omitted for brevity. The $f_{\rm prompt}$ values range between 87% and 97%, depending on the D-meson species and on the $p_{\rm T}$ interval.

The (Acc $\times\,\epsilon$) corrections were determined using Monte Carlo simulations: minimum bias pp collisions at $\sqrt{s} = 8\,$TeV were simulated with the PYTHIA v6.4.21 [14] event generator with the Perugia-0 tuning. Each event was requested to contain a c$\bar{\rm c}$ or b$\bar{\rm b}$ pair and D mesons were forced to decay in the hadronic channels of interest for the analysis. The generated particles were then transported through the apparatus using the GEANT3 [15] particle transport package. The simulations were configured in order to include the luminous region distribution and the conditions of all the ALICE subsystems, including a detailed description of their geometry and response.

The (Acc $\times\,\epsilon$) correction factor was extracted separately for both prompt and feed-down D mesons with $|y| < |y|_{\rm fid}$ as a function of $p_{\rm T}$: at low $p_{\rm T}$, (Acc $\times\,\epsilon$) are of the order of 1% or less, while they increase up to about 50% at large $p_{\rm T}$ for D$^+$ mesons and to about 80% for D^{*+} mesons. The efficiencies for D mesons from B decays are higher than those for prompt D mesons in most of the $p_{\rm T}$ intervals, because feed-down D mesons decay further from the primary vertex, due to the large B-meson lifetime ($c\tau \simeq 500\,\mu$m) [12].

The integrated luminosity was computed as $L_{\rm int} = N_{\rm ev,MB}/\sigma_{\rm MB}$, where $N_{\rm ev,\ MB}$ and $\sigma_{\rm MB}$ are the number of events and the cross section, respectively, of pp collisions passing the minimum-bias trigger condition (sect. **2**). The $\sigma_{\rm MB}$ value was obtained from the measurements of the van der Meer scans and found to be 56.4 mb ($\pm$5% systematic uncertainty).

4˙2. *Systematic uncertainties.* – Several sources of systematic uncertainty were investigated.

The systematic uncertainty on the raw yield extraction obtained from the fits of the invariant mass (mass-difference for D^{*+} mesons) distributions was determined by repeating the fit several times using i) a different binning of the histograms, ii) varied limits of the intervals for the fit range, iii) a new fit function for the background (for D^{*+} mesons, $a(\Delta M - m_\pi)^b$ instead of $a\sqrt{\Delta M - m_\pi}\exp(b(\Delta M - m_\pi))$; linear and second-order polynomial for D$^+$ mesons). Furthermore, instead of extracting the raw yield from the fit of the histogram, a method based on bin counting was used: the signal yield was obtained by integrating the invariant mass distribution after subtraction of the background estimated from a fit in the mass side-bands. The systematic uncertainty was defined as the RMS of the yields obtained in different cases.

Discrepancies between data and simulation for the variables optimised to select D-meson candidates can be an additional source of systematic error. To estimante the effect of the selected cuts on the final cross sections, the analysis was repeated with differ-

ent selection criteria (tighter and looser) and the resulting cross sections were compared. In case of D^+-meson candidates, the systematic uncertainty due to cut variation was estimated to be about 5%, except at very low p_T (10%), while for D^{*+}-meson candidates it was found to be 10% at low p_T, about 5% up to 6 GeV/c and very small ($\sim 1\%$) above 6 GeV/c, where the applied cuts are very loose.

The systematic uncertainty due to tracking efficiency was evaluated by varying the track-quality selection criteria and by studying the "matching efficiency", *i.e.* by comparing the probability of prolonging a track from the TPC inward to the ITS in data and MC. The value of the systematic uncertainty was obtained as the convolution of the uncertainties due to the two mentioned effects: it was found to be 3% per track, hence 9% for three-body decay.

The systematic uncertainty on the PID selection efficiency was estimated by repeating the analysis without applying PID and by looking at the variation of the corrected yields: the cross sections were found to be compatible with those obtained with the PID selection. Therefore, no systematic error was assigned.

Another source of systematic uncertainty is related to a possible difference between the real D-meson p_T distribution and the one assumed in the simulation, obtained from the PYTHIA 6 generator with Perugia-0 tune. A discrepancy in the p_T shape would affect the (Acc $\times$ ϵ) correction factor. To estimate the effect of the assumed p_T shape, an alternative shape was used, obtained from FONLL pQCD calculations. No significant contribution to the systematic uncertainty was found above 4 GeV/c, while at low p_T an error up to 2% was assigned.

The systematic uncertainty on feed-down estimation was extracted by considering the uncertainty on the FONLL beauty production cross section (sect. **4**·1), as well as an alternative way of using the FONLL calculations. The first method consisted in the variation of the b-quark mass, the factorisation and normalisation scales, as described in [2]. The alternative procedure was based on the ratio of the FONLL cross sections for the feed-down and prompt D mesons:

$$f_{\rm prompt} = \left(1 + \frac{(\mathrm{Acc} \times \epsilon)_{\rm feed\text{-}down}}{(\mathrm{Acc} \times \epsilon)_{\rm prompt}} \frac{\left.\frac{\mathrm{d}\sigma^{\mathrm{D\ from\ B}}_{\mathrm{FONLL}}}{\mathrm{d}p_T}\right|_{|y|<0.5}}{\left.\frac{\mathrm{d}\sigma^{\mathrm{D}}_{\mathrm{FONLL}}}{\mathrm{d}p_T}\right|_{|y|<0.5}} \right)^{-1} . \tag{3}$$

The assigned systematic uncertainty due to feed-down was calculated from the spread of the cross sections estimated with the two methods.

An additional 5% uncertainty on the minimum-bias trigger cross section and a contribution deriving from the uncertainty on the branching ratios of the considered D-meson decay channels [12], were assigned.

Table I shows a summary of all the contributions to the systematic error discussed in this section for both D^+ and D^{*+} mesons for three p_T intervals.

5. – D-meson cross sections

The p_T differential cross sections for prompt D^+-meson and D^{*+}-meson production at mid-rapidity are shown in fig. 2: the symbols are positioned horizontally at the centre of each p_T bin, with the horizontal bars representing the p_T interval width. The error bars represent the statistical uncertainties, while the systematic uncertainties are shown as boxes around the data points.

TABLE I. – *Summary of relative systematic uncertainties for three $p_{\rm T}$ intervals.*

	$\rm D^+$			$\rm D^{*+}$		
$p_{\rm T}$ (GeV/c)	1–2	6–7	16–24	1–2	6–7	16–24
Raw yield extraction	4	4	5	8	3	2
Selection efficiency	10	5	5	10	5	1
Tracking effiency	9	9	9	9	9	9
PID efficiency	0	0	0	0	0	0
$p_{\rm T}$ shape in MC	2	0	0	2	0	0
Feed down	$^{+2}_{-34}$ %	$^{+2}_{-6}$%	$^{+6}_{-13}$ %	$^{+4}_{-50}$ %	$^{+2}_{-6}$%	$^{+1}_{-8}$%
Branching ratio	2.5%			1.26%		
Normalisation	5%			5%		

The measured cross sections are compared to the FONLL predictions, a perturbative quantum chromodynamical calculation based on collinear factorisation [2,16]. The results of these calculations, performed in the same $p_{\rm T}$ intervals of the measured data, are displayed in fig. 2 as filled boxes spanning the theoretical uncertainties, estimated by varying the renormalisation and factorisation scales and by taking into account also the effect of the PDF and charm-quark mass uncertainties.

It can be noted that, while fully compatible, the measured cross section values are in the upper side of the FONLL uncertainty band, as it was already observed at lower collision energies.

Figure 3 shows the ratio of the $p_{\rm T}$ differential cross sections of $\rm D^{*+}$ and $\rm D^+$, compared to the ratio of the theoretical predictions from FONLL.

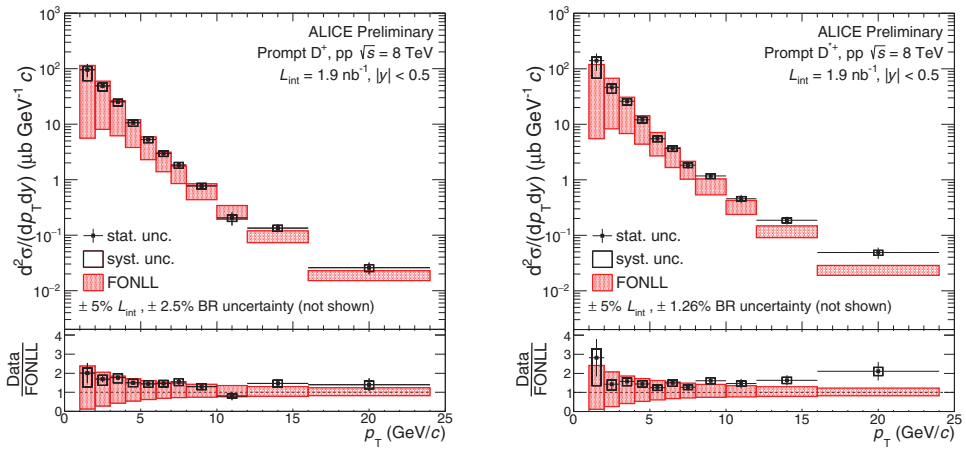

Fig. 2. – $\rm D^+$ (left) and $\rm D^{*+}$ (right) $p_{\rm T}$ differential inclusive production cross sections in pp collisions at $\sqrt{s} = 8$ TeV compared to FONLL calculations (top). Ratio of the measured cross section and FONLL calculations (bottom).

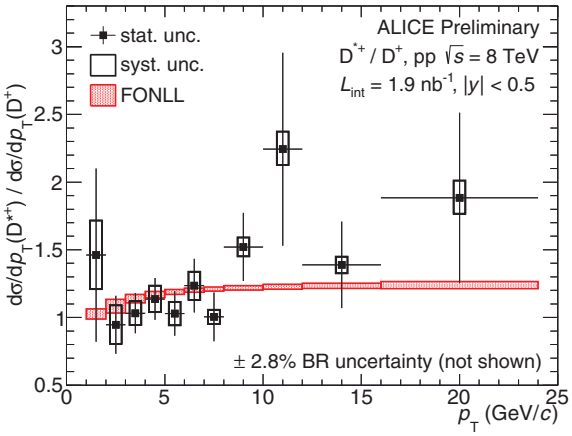

Fig. 3. – Ratio of p_{T} differential inclusive production cross section for D^{*+} / D^{+} compared to FONLL calculations at 8 TeV.

In order to evaluate the sources of the systematic uncertainties on the ratio, correlated and uncorrelated systematic effects were treated separately. In particular, the contributions from PID, tracking efficiency and normalisation uncertainties were treated as correlated between the two meson species, and in the ratio. Instead, the contributions of the feed-down from beauty-hadron decays were treated as partially correlated: the maximum and minimum values of the D^{*+}-meson cross section according to the feed-down systematic uncertainty are divided by the maximum and minimum value of the D^{+}-meson cross section. The highest resulting value is defined as the maximum value due to feed-down systematic uncertainty, and similarly for the lowest value, which is defined as the minimum one. The ratio with the central value is then considered as the systematic uncertainty of the ratio. The other contributions to the systematic errors were added in quadrature.

Concerning the uncertainties on the ratio of the theoretical predictions, all contributions to the FONLL uncertainty were treated separately. For each contribution, the uncertainty band was calculated by dividing the maximum and minumum value by the central value; the maximum deviations from the ratio of the central values defined the uncertainty band.

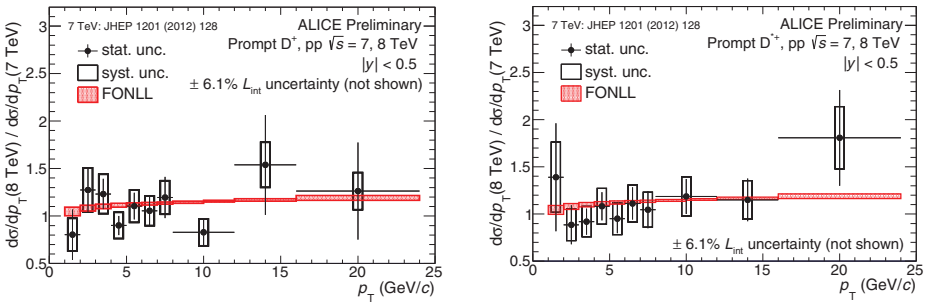

Fig. 4. – Ratio of p_{T} differential inclusive cross section at $\sqrt{s} = 8$ and 7 TeV for D^{+} (left) and D^{*+} (right), together with the ratio of the FONLL predictions.

The measured ratio of D-meson production cross sections, shown in fig. 3, does not show a significant p_{T} dependence and is compatible with the predicted ratio by FONLL.

The D-meson production cross sections at $\sqrt{s} = 8\,\mathrm{TeV}$ are compared to the analogous cross sections measured by ALICE in pp collisions at $\sqrt{s} = 7\,\mathrm{TeV}$ [17]. The ratios of these two cross sections are shown in fig. 4 for D^+ meson (left) and D^{*+} meson (right): all the contributions to the uncertainty are uncorrelated and added in quadrature, except for the feed-down contribution, which is treated as partially correlated, as for the $\mathrm{D}^{*+}/\mathrm{D}^+$ ratio.

Figure 4 shows that, in the FONLL calculation, the cross section ratio differs from unity by less than 15% in the considered p_{T} range, both for D^+ and D^{*+} mesons, and this difference is smaller than the statistical errors on the measured ratio.

6. – Summary

We have presented the measurement performed by the ALICE Collaboration of the inclusive p_{T}-differential production cross section of prompt D^+ and D^{*+} mesons at mid-rapidity ($|y| < 0.5$), in pp collisions at the centre-of-mass energy $\sqrt{s} = 8\,\mathrm{TeV}$, with p_{T} ranging from 1 to $24\,\mathrm{GeV}/c$. The mesons were reconstructed in their hadronic decay channels $\mathrm{D}^{*+} \to \mathrm{D}^0\pi^+$ $\mathrm{D}^0 \to \mathrm{K}^-\pi^+$, and $\mathrm{D}^+ \to \mathrm{K}^-\pi^+\pi^+$, and their charge conjugates.

The analysis of the decay channel $\mathrm{D}^0 \to \mathrm{K}^-\pi^+$ is ongoing.

The experimental results are reproduced within uncertainties by the theoretical predictions based on FONLL [2]; in particular, the data are in the upper side of FONLL uncertainty band, as observed also at lower centre-of-mass energy values.

Moreover, the results at $\sqrt{s} = 8\,\mathrm{TeV}$ were compared to the published ones at $\sqrt{s} = 7\,\mathrm{TeV}$ [17], showing that the cross section evolution with the centre-of-mass energy is well reproduced by the FONLL theoretical prediction. The data will be compared to recently published results on D-meson cross section in pp collisions at $\sqrt{s} = 7\,\mathrm{TeV}$ with improved precision [18].

Our results, together with existing measurements at lower energies, can provide an important contribution towards a better understanding of charm production in QCD.

REFERENCES

[1] Cacciari M., Frixione S. and Nason P., *JHEP*, **03** (2001) 006.
[2] Cacciari M., Frixione S., Houdeau N., Mangano M. L., Nason P. and Ridolfi G., *JHEP*, **10** (2012) 137.
[3] Kniehl B. A., Kramer G., Schienbein I. and Spiesberger H., *Phys. Rev. D*, **71** (2005) 014018.
[4] Kniehl B. A., Kramer G., Schienbein I. and Spiesberger H., *Eur. Phys. J. C*, **41** (2005) 199.
[5] Kniehl B. A., Kramer G., Schienbein I. and Spiesberger H., *Eur. Phys. J. C*, **72** (2012) 2082
[6] ALICE Collaboration (Aamodt K. *et al.*), *JINST*, **3** (2008) S08002.
[7] ALICE Collaboration (Abelev B. B. *et al.*), *Int. J. Mod. Phys. A*, **29** (2014) 1430044.
[8] ALICE Collaboration (Abbas E. *et al.*), *JINST*, **8** (2013) P10016.
[9] ALICE Collaboration (Aamodt K. *et al.*), *JINST*, **5** (2010) P03003.
[10] ALICE Collaboration (Alme J. *et al.*), *Nucl. Instrum. Methods A*, **615** (2010) 316.
[11] ALICE Collaboration (Adam J. *et al.*), `arXiv:1610.03055 [physics.ins-det]`.
[12] Particle Data Group Collaboration (Patrignani C. *et al.*), *Chin. Phys. C*, **40** (2016) 100001.

[13] Lange D. J., *Nucl. Instrum. Methods A*, **462** (2001) 152155.
[14] Sjöstrand T., Mrenna S. and Skands P., *JHEP*, **05** (2006) 026.
[15] Brun R., Bruyant F., Carminati F., Giani S., Maire M., McPherson A., Patrck G. and Urban L., Technical report, CERN, 1994.
[16] Cacciari M., Greco M. and Nason P., *JHEP*, **05** (1998) 007.
[17] ALICE Collaboration (Abelev B. I. *et al.*), *JHEP*, **01** (2012) 128.
[18] ALICE Collaboration (Acharya A. *et al.*), arXiv:1702.00766.